Lateral coupling of $In_xGa_{1-x}As/GaAs$ quantum dots investigated using differential transmission spectroscopy

K. L. Silverman and R. P. Mirin
Optoelectronics Division, National Institute of Standards and Technology, Boulder, Colorado 80305, USA

S. T. Cundiff
JILA, National Institute of Standards and Technology and University of Colorado, Boulder, Colorado 80309, USA
(Received 23 March 2004; revised manuscript received 24 June 2004; published 8 November 2004)

Coupling between InGaAs/GaAs quantum dots is investigated using differential transmission spectroscopy. Two-color pump-probe techniques are used to spectrally resolve the carrier dynamics, revealing carrier transfer between quantum dots at room temperature. The time constant for this process is shown to increase from 35 ps at room temperature to 130 ps at 230 K.

DOI: 10.1103/PhysRevB.70.205310 PACS number(s): 78.67.−n, 78.47.+p

Self-assembled semiconductor quantum dots (QDs) are remarkably flexible structures that are impacting many areas of optoelectronics. At low temperatures, they exhibit atomiclike properties due to their three-dimensional electronic confinement and are promising for such applications as quantum computing and cryptography. Self-assembled QDs have also proven useful when incorporated into conventional devices such as semiconductor lasers and amplifiers. Unfortunately, many of the major device improvements anticipated due to the unique QD density of states have not been realized. This is due in part to the as yet unavoidable size distribution in QD ensembles, but also due to the significant temperature-dependent coupling of individual QD transitions. Temperature-dependent coupling affects the threshold current density in QD lasers[1] and limits the isolation between channels in a QD semiconductor optical amplifier and other multichannel devices.[2,3]

Coupling between QDs in optoelectronic devices occurs via both electromagnetic and electronic mechanisms. The former couples all QDs within a homogeneous linewidth of the individual transition. The latter can couple all QDs within the inhomogeneous linewidth as electrons and holes move between QDs with different ground state energies. Each of these effects can result in Fermi level pinning and, therefore, explain the observed single-mode operation of QD lasers at room temperature.[4] In actuality, both of these processes contribute to the collective action of QD ensembles and can be difficult to distinguish. Recently, coupling in self-assembled QD ensembles has been studied extensively. The room temperature homogeneous broadening of the transition has been measured by four wave mixing[5] and single QD emission[6,7] with values ranging from a few nanometers up to more than 10 nanometers. Electronic coupling of QDs via thermal emission and subsequent recapture has been inferred from temperature dependent continuous-wave[8,9] and time- resolved[10,11] photoluminesence (PL) measurements. Unfortunately, this method relies on numerous assumptions and a multivariable fit to a series of data. Results from resonant differential transmission (DT) measurements[12,13] show an initial fast recovery of the QD absorption indicating that carriers are quickly leaving the states that they were initially created in. These experiments cannot determine whether the resonantly excited carriers are moving to other QDs or different states of the same QD.

This paper is orginized as follows. Section I contains information on the growth and preparation of the sample as well as the experimental methods employed for this study. Section II contains room temperature DT measurements including a two-color measurement capable of resolving the carrier dynamics in QDs resonant and nonresonant with pump excitation. In Sec. III we investigate the process of carrier heating that leads to electronic coupling using temperature-dependent degenerate DT measurements.

I. SAMPLE PREPARATION AND EXPERIMENTAL METHODS

The sample used in this experiment is a single layer of InGaAs/GaAs self-assembled QDs embedded in a semiconductor wave guide grown by molecular beam epitaxy. The dot layer is nominally 13.4 monolayers of $In_{0.45}Ga_{0.55}As$ grown at a substrate temperature of 520 °C positioned at the center of a 270 nm $Al_{0.10}Ga_{0.90}As$ wave-guide core, clad on both sides with 1.1 μm of $Al_{0.70}Ga_{0.30}As$. We etch 3 μm wide stripes in the top cladding layer and the wave guide is cleaved, giving a length of approximately 1 mm. The entire structure is undoped to minimize the contribution of free carrier absorption to modal loss and eliminate the effects of a built-in electric field on the carrier dynamics. A single-layer HfO_2 antireflection coating is deposited on the output facet to eliminate Fabry-Perot effects. Figure 1 contains time-integrated (PL) and absolute absorption data from this sample. It has a ground state absorption peak at 1210 nm with a full-width at half-maximum of 62 nm. Transmission electron microscopy performed on a sample from an adjacent piece on the same wafer with the top cladding etched off revealed an areal dot density of approximately 1.9×10^{10} cm^{-2}. More detailed information can be found elsewhere.[14]

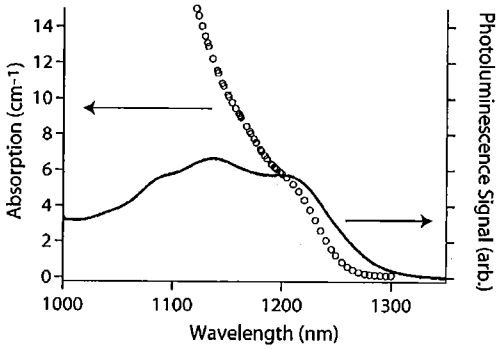

FIG. 1. Room temperature photoluminescence and absorption data for the QD wave-guide sample used in the differential transmission measurements.

For these measurements we use a wave guide to increase the interaction length with the weakly absorbing QDs. The main disadvantage of using the wave-guide geometry is the added difficulty of separating pump and probe beams after they travel colinearly and copolarized through the wave guide (QD ground state absorption occurs only in the TE wave-guide mode[14]). In the experiments presented in this paper, we use two different methods for isolating the probe beam. In both methods we employ a synchronously pumped optical parametric oscillator (OPO) to generate optical pulses resonant with the QD ground state absorption.

We use an optical gating techique for all degenerate measurements presented in this paper. For this scheme, the probe is separated from the pump by means of a nonlinear optical gate. The residual of the Ti:sapphire light used to pump the OPO is combined with the output of the QD wave guide in a sum-frequency crystal (1.5 mm of BBO). The gating pulse and the probe pulse are on fixed delay lines with identical path lengths and generate a sum-frequency signal proportional to the probe intensity. The pump beam is on a variable delay line, to allow the time between pump and probe arrival to be varied. The optical delay of the pump beam is, for the most part, different from the probe and gate delays. Therefore, the pump beam does not contribute to the sum-frequency signal detected by a photomultiplier tube, allowing background-free detection of the probe. The only problem occurs around zero path difference, where the pump, probe, and gate all have identical delays. Here, the pump generates an intense sum-frequency signal, obscuring the DT for delay times less than about 500 fs. The QD wave-guide sample is mounted in an optical cryostat with a short working distance to allow the use of high numerical aperture microscope objectives for input and output coupling, and the temperature is monitored by a calibrated silicon diode mounted in close contact with the sample.

For two-color DT measurements we implement an RF chopping scheme to increase our signal-to-noise over the previous technique. The pump beam is chopped at low frequency and sent to a zero-dispersion pulse shaper. The pulse shaper allows us to reduce the bandwidth of the pump beam and select its center frequency within the spectrum of the OPO. The probe beam is modulated at 1 MHz by an acousto-optic modulator (AOM) and is coupled into the wave guide, retaining the full OPO bandwidth. After interaction with the sample, the light is sent to a spectrometer and detected with an InGaAs photodiode. The probe beam is then demodulated with an RF lock-in amplifier, and the DT signal is detected at the pump chop frequency with a conventional lock-in. This method allows us to observe the evolution of the DT signal for QDs resonant and nonresonant with the pump excitation. One drawback of this technique is that it exhibits a signal for negative time delay since the probe beam's effect on the pump is present at the detection frequency. Other than making the baseline signal more difficult to determine, this does not hinder measurements of the relevant relaxation times.

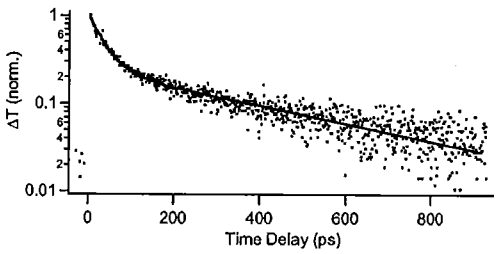

FIG. 2. Room temperature degenerate DT trace at 1225 nm (dots) along with a biexponential fit to the data (solid line).

II. ROOM TEMPERATURE MEASUREMENTS

Figure 2 shows a 295 K DT scan taken on the ground state transition of our QD wave-guide sample. The pump-:probe ratio was 10:1, and we insured that the carrier density was much less than one electron-hole pair per dot by comparing excitation levels with intensity-dependent absorption measurements of this sample.[14] For time delays greater than 1 ps, the curve clearly involves two separate time constants. When fit with a sum of two exponential decays, a shorter time constant of 34±3 ps and a longer time constant of 450±30 ps are obtained. The initial time constant represents heating of the resonantly excited carriers and has been observed by other groups. The thermalization time reported in these references ranges from 6 ps (Ref. 12) up to 65 ps (Ref. 13) with the general trend being longer time constants for larger dots. The literature is not clear on whether these carriers are being thermalized to excited states of the dot in which they were initially created or if they escape their original QD and are recaptured by other QDs. The longer time constant represents the radiative decay of the thermalized carrier population and is in general agreement with radiative lifetimes measured by time-resolved PL.

To gain a better understanding of the spectral diffusion of resonantly excited electron-hole pairs, two-color measurements are performed. Figure 3 shows the spectrally resolved DTS on the ground state of the QDs at various fixed delays between pump and probe. The pump beam was spectrally filtered to a bandwidth of ≈2 nm. At small pump-probe time delays, the DT signal indicates a spectral hole centered on, but much larger than the pump bandwidth. We believe that the width of this initial signal (12±1 nm FWHM) is repre-

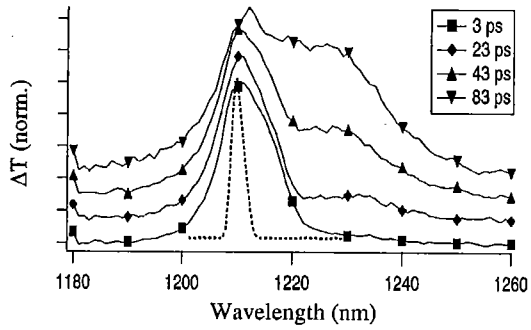

FIG. 3. Spectrally resolved DT at 295 K at various fixed delay times. Pump spectrum is indicated by the dashed curve and traces are offset for clarity.

sentative of the homogeneous linewidth of the QDs, and it is in reasonable agreement with data from four-wave mixing and single-dot photoluminescence.[5–7] As the delay is increased, a signal is observed at wavelengths outside the initial spectral hole. This nonresonant signal increases in intensity with increased probe delay until it is the dominant contributer to the overall DT signal. To better quantify the very different carrier dynamics occuring at the various probe wavelengths, time-resolved measurements at fixed wavelength were performed and are included in Fig. 4. Figure 4(a) data was taken at a spectral position covered by the initial spectral hole but not resonant with the pump excitation. The DT in this case exhibits the same biexponential decay representative of carrier heating and radiative recombination as the data collected in the resonant experiment above. When the probe detection window is moved off of the initial spectral hole induced by the pump, as in Fig. 4(b), the DT exhibits no signal at zero delay indicating that the states being probed are initially empty. The DT then rises to a peak at approximately 60 ps before decaying with a much larger time constant. A least squares fit to this signal (not shown) yields a risetime of 35 ps. Since the risetime of the nonresonant signal and the decay time of the resonant signal are almost identical, we can conclude that the source of the carriers filling the nonresonant states is indeed the resonantly excited carriers. Also, the energy separation between pump excitation and probe detection is much smaller than the energy spacing between the ground and excited state of these QDs. This precludes intradot effects as the origin of the nonresonant DT signal. Considering the arguments above, it is clear that carrier transfer between QDs is occurring at room temperature.

Other groups have carried out similar experiments on self-assembled QDs. Akiyama *et al.*[2] report spectral hole burning on vertically coupled QDs. Their experiment yields a homogeneous broadening of 12 nm, in agreement with our results, but does not resolve the carrier transport between QDs. Urayama *et al.*[15] also report spectrally resolved DT on vertically coupled QDs. Their results are at 10 K and indicate a large spectral hole (>20 nm) at times less than a picosecond which they attribute to vertical coupling of QDs. Since our experiment was performed on a single layer of QDs, vertical coupling is not an issue, and the relatively small spectral hole in our data lends some credence to their group's vertical

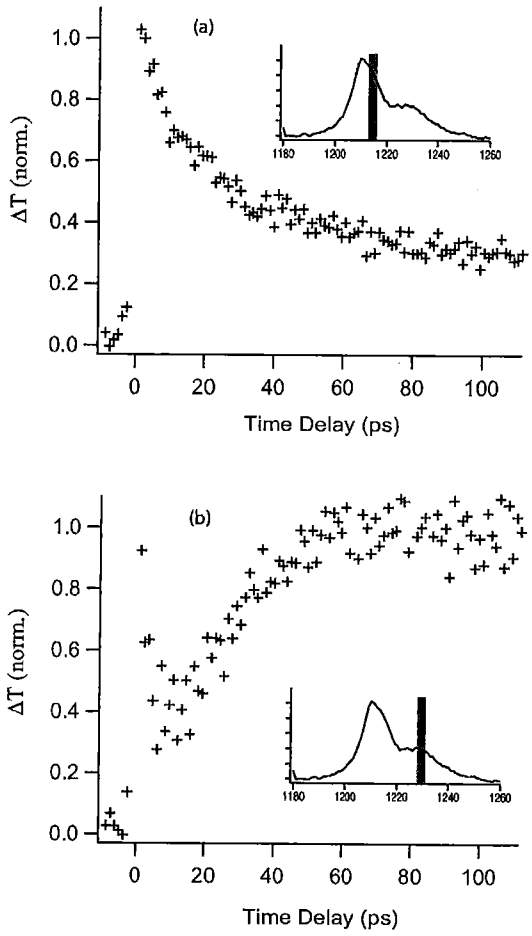

FIG. 4. Time-resolved DT traces for the QD wave-guide sample. The shaded region of the inset indicates the spectral region of probe detection with respect to the spectrally resolved DT at a fixed delay of 43 ps. The probe wavelength and bandwidth is identical to that used in Fig. 3.

coupling theory. The fact that Akiyama *et al.* do not see vertical coupling in their data is surprising, but may have something to do with the details of the barrier length and material between QDs. Also, since the measurements of Urayama *et al.* were performed at low temperature, coupling between QDs in the same layer was not observed.

III. TEMPERATURE DEPENDENT MEASUREMENTS

In order to gain some understanding of the process associated with carrier escape from the QDs, temperature dependent DT on the ground state was performed. To insure that DT is performed at a consistent position in the QD inhomogeneous linewidth, we adjust the wavelength of the laser light to track the temperature-dependent ground state energy. For each temperature, a low intensity PL spectrum is first taken, and the laser wavelength is chosen to be where the PL amplitude is $\frac{2}{3}$ of its peak on the low energy side. Therefore, the energy barrier for carrier escape and the influence of excited states on the DT is similar at each temperature point.

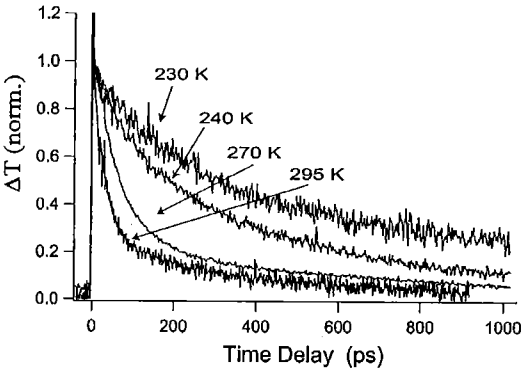

FIG. 5. Temperature-dependent DT data taken on the ground state of the QD sample. Measurements were taken at low excitation. The laser wavelength was determined by temperature-dependent PL measurements.

DT measurements taken at low pump powers and different sample temperatures are displayed in Fig. 5. As the sample temperature is decreased from 295 K to 230 K, the short time constant increases dramatically. The longer time constant remains relatively constant over this temperature range. We fit the different temperature DT scans with a biexponential function and a least-squares fitting routine. The temperature dependence of the carrier escape time is shown in Fig. 6. Below 230 K the DT signal becomes monoexponential, indicating minimal carrier escape from the QDs. Since we are mainly interested in the carrier escape process, we only discuss the DT for temperatures 230 K and above.

The strong temperature dependence of the escape rate over this temperature range, along with the large potential barrier for escape in our dots (>100 meV), suggests absorption of longitudinal optic (LO) phonons as the mechanism.[16,17] The question then is whether to model the interaction as thermal or multiphonon escape. A thermal interaction is appropriate if the QDs have a continuous or quasicontinuous density of states (DOS), where as a discrete transition requires a multiphonon approach. Without detailed knowledge of the QD DOS it is unclear which model will correctly predict our escape time and justification for both

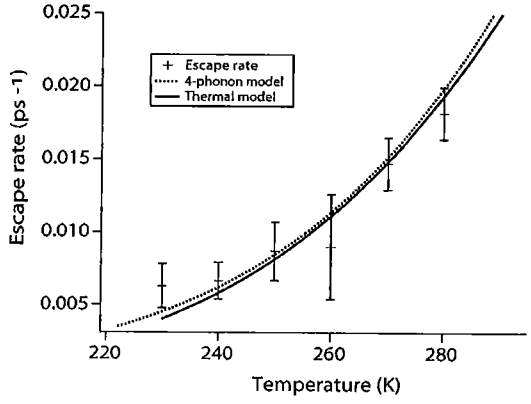

FIG. 6. Carrier escape rate as a function of temperature obtained from biexponential fits to the data in Fig. 5. Included on the graph is Eq. (1) with $n=4$ and Eq. (3) with $E_a=175$ meV.

methods can be found in the literature. Temperature dependent DT measurements with nonresonant pumping,[18] time-resolved PL,[19] and photoluminescence excitation (PLE)[20] experiments reveal that carrier capture proceeds by multiphonon emission at low carrier densities, lending credence to the multiphonon approach. On the other hand, a thermal model correctly predicts the time-resolved and time-intergrated PL from some QD samples.[8,9] Therefore, we fit our temperature dependence with both approaches.

For the multiphonon interaction we have

$$\frac{1}{\tau} \propto [N_{\mathrm{LO}}(T)]^n, \tag{1}$$

with

$$N_{\mathrm{LO}} = \frac{1}{\exp\left(\frac{E_{\mathrm{LO}}}{kT}\right) - 1}, \tag{2}$$

where τ is the carrier escape time, N_{LO} is the Bose-Einstein distribution function for LO phonons, E_{LO} is the LO phonon energy taken here to be 32 meV (Ref. 20) and n is the number of phonons involved in the transition. We limit ourselves just to LO phonon interaction for two reasons. First, the interaction with LA phonons is considerably weaker.[16] Second, the temperature dependence of the longitudinal acoustic (LA) phonon density is basically flat at room temperature and, therefore, including this in the overall model has only a small effect. LA phonons are expected to play an important role for energy conservation at lower sample temperatures due to the very sharp transitions of cold self-assembled QDs.[16] The temperature dependence of the thermal escape process can be modelled as

$$\frac{1}{\tau} \propto \exp^{-E_a/kT}, \tag{3}$$

where E_a is an activation energy to an unconfined state.

As seen in Fig. 6, both equations can be made to fit our data effectively within our experimental uncertainty, and therefore we are not able to rule out either process. The multiphonon model fits best with a 4 LO phonon process yeilding a 128 meV energy separation between initial and final scattering states. The thermal model, on the other hand, gives us an activation energy of 175 meV. The actual barrier for escape in these QDs probably lies somewhere in between these two limiting cases.

In our sample, the separation between the ground state transition and the wetting layer is approximately 300 meV, and is about two times the escape energies determined from the fits to the experimental data. This indicates a single carrier escape to the wetting layer. Determining the charge of the carrier is more complicated especially considering the uncertainty of the band offset parameter in these structures.[21] One can find experimental evidence for both electron[24] and hole[22,23] escape as the dominant contribution to the process. Further experiments are necessary to resolve this apparent contradiction.

In summary, we have investigated the process of carrier transfer between self-assembled QDs near room temperature.

By employing two-color differential transmission we were able to conclusively determine that carrier transfer occurs between QDs resonant with pump excitation and those initial empty with a time constant of approximately 35 ps. In addition, the width of the initial spectral hole in this experiment gives an estimate of 12 nm for the homogeneous broadening in our InGaAs/GaAs QDs. The temperature dependence of the escape rate was also measured using degenerate DT spectroscopy. The time constant for this process was shown to increase strongly with decreasing temperature indicating escape to the QD wetting layer.

ACKNOWLEDGMENT

We acknowledge Todd Harvey for growth of the sample.

[1] D. L. Huffaker, G. Park, Z. Zou, O. B. Shchekin, and D. G. Deppe, Appl. Phys. Lett. **73**, 2564 (1998).
[2] T. Akiyama, H. Kuwatsuka, T. Simoyama, Y. Nakata, K. Mukai, and M. Sugawara, IEEE Photonics Technol. Lett. **12**, 1301 (2000).
[3] M. Grundmann, F. Heinrichsdorff, C. Ribbat, and D. B. M.-H. Mao, Appl. Phys. B: Lasers Opt. **69**, 413 (1999).
[4] M. Sugawara, K. Mukai, and Y. Nakata, Appl. Phys. Lett. **74**, 1561 (1999).
[5] P. Borri, W. Langbein, J. Mork, J. M. Hvam, F. Heinrichsdorff, M.-H. Mao, and D. Bimberg, Phys. Rev. B **60**, 7784 (1999).
[6] M. Bayer and A. Forchel, Phys. Rev. B **65**, 041308 (2001).
[7] K. Matsuda, T. Saiki, H. Saito, and K. Nishi, Appl. Phys. Lett. **76**, 73 (2000).
[8] A. Patane, A. Levin, A. Polimeni, L. Eaves, P. Main, M. Henini, and G. Hill, Phys. Rev. B **62**, 11 084 (2000).
[9] S. Sanguinetti, M. Henini, M. G. Alessi, M. Capizzi, P. Frigeri, and S. Franchi, Phys. Rev. B **60**, 8276 (1999).
[10] F. Pulizzi, A. J. Kent, A. Patane, L. Eaves, and M. Henini, Appl. Phys. Lett. **84**, 3406 (2004).
[11] W. Yang, R. R. Lowe-Webb, H. Lee, and P. C. Sercel, Phys. Rev. B **56**, 13 314 (1997).
[12] P. Borri, E. Langbein, J. M. Hvam, F. Heinrichsdorff, M.-H. Mao, and D. Bimberg, IEEE J. Sel. Top. Quantum Electron. **6**, 544 (2000).
[13] D. Birkedal, J. Bloch, J. Shah, L. N. Pfeiffer, and K. West, Appl. Phys. Lett. **77**, 2201 (2000).
[14] K. L. Silverman, R. P. Mirin, and S. T. Cundiff, Appl. Phys. Lett. **82**, 4552 (2003).
[15] J. Urayama, T. B. Norris, B. Kochman, J. Singh, and P. Bhattacharya, Appl. Phys. Lett. **76**, 2394 (2000).
[16] T. Inoshita and H. Sakaki, Phys. Rev. B **46**, 7260 (1992).
[17] N. Del Fatti, P. Langot, R. Tommasi, and F. Vallee, Proc. SPIE **3277**, 96 (1998).
[18] J. Feldmann, S. T. Cundiff, M. Arzberger, G. Bohm, and G. Abstreiter, J. Appl. Phys. **89**, 1180 (2001).
[19] R. Heitz, H. Born, T. Luttgert, A. Hoffmann, and D. Bimberg, Phys. Status Solidi B **65**, 65 (2000).
[20] R. Heitz *et al.*, Appl. Phys. Lett. **68**, 361 (1996).
[21] L. Chu, A. Zrenner, G. Bohm, and G. Abstreiter, Appl. Phys. Lett. **76**, 1944 (2000).
[22] W. H. Chang, T. Hsu, C. C. Huang, S. L. Hsu, C. Y. Lai, N. T. Yeh, T. E. Nee, and J. I. Chyi, Phys. Rev. B **62**, 6959 (2000).
[23] W. H. Chang, W. Y. Chen, T. Hsu, N. T. Yeh, and J. I. Chyi, Phys. Rev. B **66**, 195337 (2002).
[24] P. N. Brunkov, A. Patane, A. Levin, L. Eaves, P. C. Main, Y. G. Musikhin, B. V. Volovik, A. E. Zhukov, V. M. Ustinov, and S. G. Konnikov, Phys. Rev. B **65**, 085326 (2002).